33RD CONGRESS
OF THE INTERNATIONAL COUNCIL
OF THE AERONAUTICAL SCIENCES
STOCKHOLM, SWEDEN, 4-9 SEPTEMBER, 2022

ICAS 2022 SWEDEN

DEVELOPING A DEPARTURE QUEUE MODEL FOR INTEGRATED ARRIVAL AND DEPARTURE OPERATION OF RUNWAYS

Eri Itoh[1, 2], Daiki Iwata[1] & Michael Schultz[3]

[1]Department of Aeronautics and Astronautics, The University of Tokyo, Tokyo 113-8656, Japan
[2]Air Traffic Management Department, Electronic Navigation Research Institute, Tokyo 182-0012, Japan
[3]Institute of Flight Systems, Bundeswehr University Munich, 85577 Neubiberg, Germany

Abstract

Reducing the length of departure queues at runway entry points is one of the most important requirements for de- creasing air traffic congestion. This study designeds an aircraft departure model for arrival traffic interference at runways using a time-varying fluid queue. The proposed model enables us to estimate the aircraft waiting time in the departure queue, and evaluate the impact of arrival traffic at a related runway. As a case study, this paper models the departure queue at runway 05 of Tokyo International Airport during an entire day of operations and applies the arrival traffic influence of runway 34R to the model. Using actual traffic data of departures and suppositions of additional arrival aircraft, the model quantitatively clarified that aircraft experience increasing departure waiting time on days at runway 05 due to arrival traffic at runway 34R without integrated arrival and departure air traffic management.

Keywords: data analysis, queuing theory, airport operations, runway management, departure air traffic

1. Introduction

Congestion reduction at major airports improves operational efficiency and safety while also reducing fuel consumption and delays for arriving and departing air traffic. When runways have limited capacity, this causes a bottleneck for all air traffic. Thus, integrating arrival and departure aircraft traffic management at the runway is effective for accommodating increasing air traffic demand while mitigating air traffic congestion in and around the airport. The characteristics of the air traffic depend on airport-specific aspects such as runway configurations, taxiways, aprons/ramps, gates, and terminal buildings, as well as the geometrical and operational constraints at the surface and in the surrounding airspace.

Airports is aircraft departure management is a key operation for airports, and "departure metering," which assigns suitable holds for departure aircraft at their gates [1, 2], is particularly important. The goal of departure metering is to reduce the departure queue at runway entry points while maintaining the runway throughput [3]. As far as the authors are aware, there have been few studies characterizing the stochastic features of the aircraft departure process.

To predict aircraft waiting times at a departure queue, several studies propose queuing models to analyze the taxi-out process of the departure air traffic [3, 4, 5]. In Reference [4], the authors express a single departure runway queue using$D(t)/E_k(t)/1$ queuing model, assuming that the aircraft arrive at the queue according to a time-dependent schedule and that the service rate follows a time-dependent Erlang distribution. In Reference [5], the authors model airport surface operations of departure air traffic from a single ramp to multiple departure runways using a fluid-flow queuing model. The expected queue length is determined using the flow conservation principle. These queuing networks were used to estimate taxi-out times at three case study airports in the United States [3]. The results showed that the taxi-out times of 60% to 70% flights were estimated within a margin of error of 5 minutes. The accuracy of these estimates, however, impacts the performance of departure metering.

For example, departing aircraft take off from takeoff-only runways approximately every two minutes at Tokyo International Airport (RJTT). Thus, For this reason, estimation margin of error should be less than a minute in order to minimize the departure queue at the runway entry point. Furthermore, we need a departure queue model which allows us to input the time-varying number of departure aircraft entering the runway in a unit time to achieve integrated arrival and departure control. This departure queue model should also enable us to estimate the optimal departure rate at the runway entry points and to control time-varying arrival and departure rates at the runway approximately 30 to 40 minutes before the corresponding landing and takeoff.

With this background in mind, this study took on the challenge of proposing a new departure metering approach for integrated arrival and departure management. To improve accuracy, the push-back and taxi time are estimated using a Machine Learning (ML) model. Based on these times, the departure queue is estimated at the runway entry points. The spot-out time of departure aircraft is controlled to maintain the ideal departure rate at the runway entry point to minimize the estimated departure queue. In this paper, we developed departure queue model [8] which allows us to input the actual time-varying departure rate and estimate the departure queue for integrated arrival and departure operations. The departure queue model applies $G(t)/GI/s(t)$ fluid queues [6, 7] assuming a single server, where the arrival and service processes of the queuing system follow general distributions. In our model, the number of servers corresponds to the rate of runway usage. The $G(t)/GI/s(t)$ queue allows us to model time-varying arrival rates and varying numbers of servers (i.e., available runway capacity), using realistic assumptions when considering the management of departing traffic at airports. In the process of developing our proposed time-varying fluid queue into a multi-server model, this paper examines the aircraft departure waiting time under interference of arrival air traffic at a single runway. Based on the analytical results, we discuss the potential of integrated arrival and departure air traffic management at single runway operations.

Incoming and outgoing air traffic at airports is typically modeled using queuing models. Reference [9] provided a wide-ranging review of the literature on stochastic modeling applications within aviation including past studies on the formulation of queuing systems for air traffic. These studies suggested that developing data-driven and stochastic modeling approaches according to empirical data could be one of the most valuable research opportunities in this research area. In line with this, one of the authors used operational data and modeled arrival air traffic by comparing estimation results against actual data. In Reference [10], the arrival delay at an airport is analyzed using a $G/G/c$ queuing model, using data from two years of radar tracks and flight plans from Tokyo International Airport (RJTT). A shift from traffic flow to arrival time management here indicates capacity enhancements. This initial approach was improved [11] by considering extended arrival management. Approaching the airport, the management of the required inter-arrival times between assigned aircraft (minimum separation standards) and airspace capacities are limiting constraints. The analysis identifies bottleneck areas where the efficient management of inter-arrival times could mitigate operational delays. The focus of Reference [12] was the evaluation of different tactical control strategies for RJTT arrivals 100 NM around the airport using the proposed queuing in comparison to a $M/G/c/K$ queuing model. In this study, an improved arrival strategy was suggested considering service times and variances of service times in the airspace areas. The effectiveness of the proposed arrival strategy was verified using an agent-based simulation study [13].

However, these queuing models assumed a steady state. In this study, we designed an aircraft departure traffic model for runway entry points using $G(t)/GI/s(t)$ fluid queue, with time-varying departure rate and available runway capacity. We demonstrate our model for RJTT departure runway 05 under arrival interference at runway 34R in this paper. Using actual traffic data of departures at runway 05 and assuming increasing arrival air traffic at runway 34R in future operations, the model quantitatively clarified that aircraft experience increasing departure waiting time due to increasing arrival interference without integrated arrival and departure air traffic management at multiple runways at the target airport.

This paper is organized as follows. Section 2 introduces the airport operations at RJTT and explains the influence of arrival traffic on runway 05 departures. The analysis considers recorded aircraft track data for 36 days of operations. This data was recorded in 2019 and 2020 before COVID-19 required the introduction of restrictions on air traffic. Section 3 introduces a $G(t)/GI/s(t)$ fluid queue for the aircraft departure traffic at runway 05. Section 4 applies the model to an entire day of departure traffic at runway 05 and estimates the waiting time of the aircraft in the departure queue there. In addition, we expand the model to include the impact of arrival traffic and compare the estimates for waiting time. In Section 5, we discuss future extension of the model to departure and arrival mixed runways. Finally, Section 6 outlines our future works and provides conclusions.

2. Data Analysis of the Surface Operations

2.1 Airport Operation at Tokyo International Airport (RJTT)

RJTT is Japan's largest airport in terms of the number of runways, of which it has four. From the viewpoint of passengers, RJTT is the world's fourth busiest airport [14]. Figure 1 shows an airport map of RJTT.

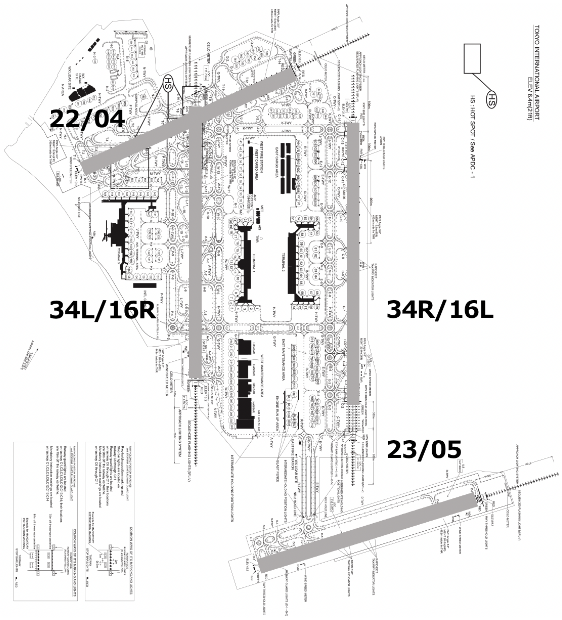

Figure 1 – RJTT surface configuration [15].

As you can see from Figure 1, the runway configuration at RJTT features parallel crosses with two north-to south runways (34L/16R and 34R/16L) and two southwest-to-northeast crosswind runways (22/04 and 23/05). The runways used depends on the wind direction. In northerly wind conditions, aircraft arrive at either runway 34L or runway 34R, and departing aircraft takeoff from either runway 05 or runway 34R depending on their origin and destination airports. Runway 05 is used only for departure operation, allowing a maximum of 28 departures per hour. Runway 34R is used as a departure and arrival mixture runway. This runway allows a maximum of 12 departures per hour. Figure 2 shows the runway usage for departures and arrivals at RJTT in the northerly wind conditions. In the southerly wind conditions, the arrival runway used is either runway 16R or runway 16L, and traffic departures are from runway 22, 16R or 16L. The operation that arrival traffic use runway 34L or runway 34R, departure traffic use runway 05 or 34R comprise a large percentage of the airport's operations, about 70%. In this paper, we focus on the northerly wind condition operations, especially the runway used only for departures, runway 05.

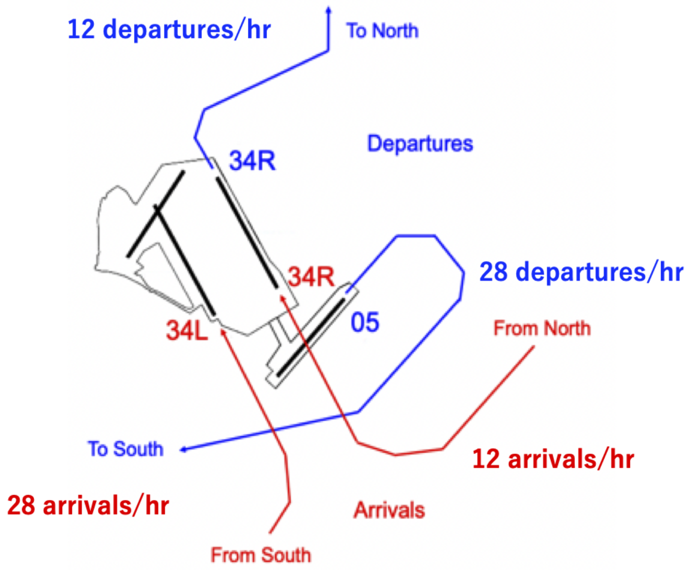

Figure 2 – RJTT northerly wind operations

This paper uses 36 days of actual radar data recorded between September 2019 and February 2020, the same data as used in previous work [8]. This radar data consists of departure and arrival aircraft trajectories including time, latitude, longitude, and altitude on the surface and at approach and climb phases at each second for corresponding aircraft types and call signs. All data was provided by the Japan Civil Aviation Bureau (JCAB) of the Japanese Ministry of Land, Infrastructure, Transport, and Tourism for limited use in this study. Figure 3 shows aircraft track data on the RJTT surface departing from runway 05 in a single day.

Figure 3 – RJTT departures from runway 05

2.2 Arrival and Departure Traffic Interference at RW05

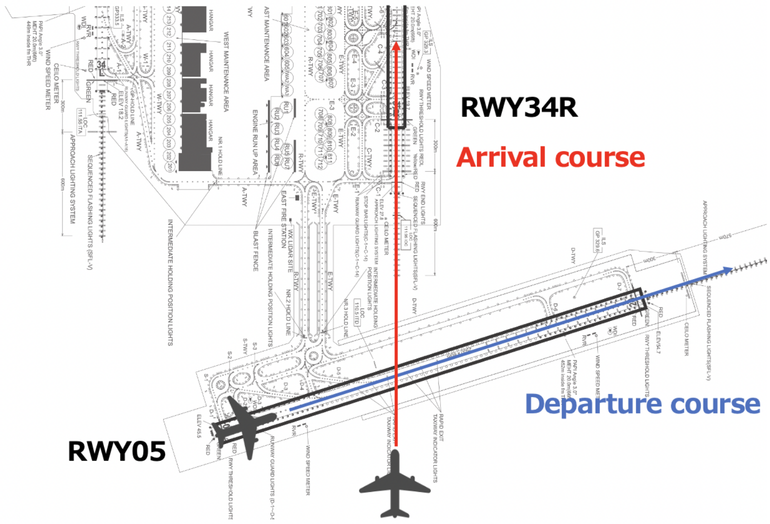

Figure 4 – Positional relationship between Runway 05 and Runway 34R.

RJTT's runway 05 is used only for departures in northerly wind conditions. However, this does not mean there is no inference from arrival aircraft. Figure 4 shows the positional relationship between runways 05 and runway 34R. In northerly wind conditions, runway 34R is used for departure and arrival traffic. This means that runway 34R arrival aircraft flies over a portion of runway 05. Accordingly, runway 05 departures cannot start their takeoff when runway 34R arrivals are approaching the airport until this arrival traffic passes through the point at the intersection of the runway 34R landing course and runway 05, due to the rules of runway operation. Consequently, runway 34R arrival traffic interferes with runway 05 departures.

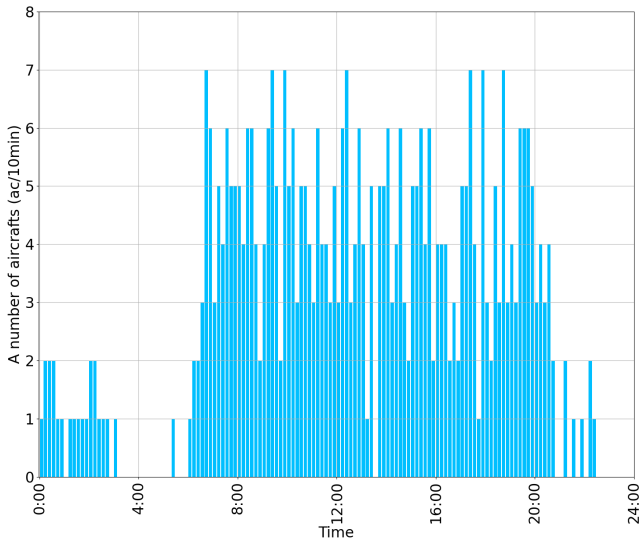

Figure 5 – Distribution of runway 05 departure for a single day.

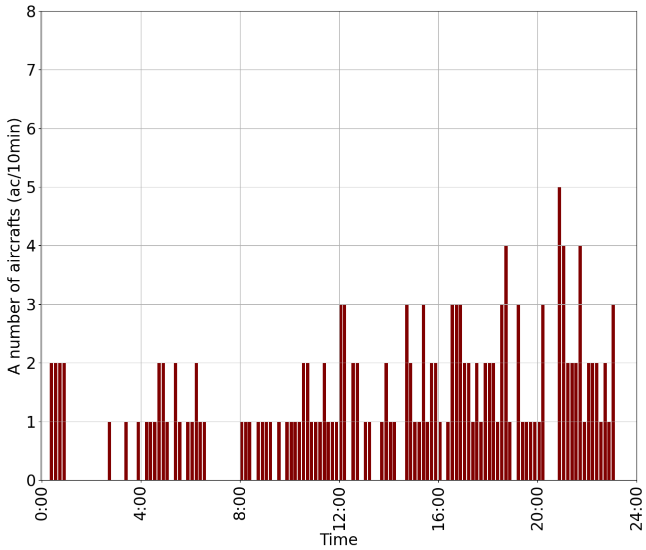

Figure 6 – Distributions of runway 34R arrival for a single day.

Figures 5 and 6 show the distributions of runway 05 departures and runway 34R arrivals in a single day. These figures show that there are many instances in which runway 05 departures and runway 34R arrivals are occurring concurrently.

3. Model Description and Formulation

3.1 Modeling Departure Queue at RW05

This study describes the aircraft departure queue at a single runway, runway 05 at RJTT, by means of a $G(t)/GI/s(t)$ fluid queue model as follows. The entrance to the queuing system is the point on the taxiways 0.5 NM from the runway entry points. In addition, the exit of the queuing system is the departure runway end. Thus, our model covers the runway and taxiway within 0.5 NM distance from the runway entry points, as in prior research [8]. In addition, we include the impact of runway 34R arrivals on the queuing system as illustrated in Figure 7.

Time-varying arrival rate $\lambda(t)$ is counted from the point the departure aircraft enter the queuing system 0.5 NM away from the runway 05 entry points. Accordingly, the inter-arrival time is defined as the time between two consecutive departure aircraft entering the system. Service time is given as the sum of Runway Occupancy Time (ROT) and spacing time with the proceeding departure aircraft at the runway entry points. The number of servers $s(t)$ is defined as the number of departure aircraft which are allowed to use the runway. In this paper, $s(t)$ is given as a time-varying parameter, particularly, $s(t) = 1.0$, when the runway 34R arrival traffic state is the same as actual data. If the modeled runway 34R arrival rate is higher than the actual rate, $s(t) < 1.0$ in contrast. The determinant procedure details are described in Section 4.2

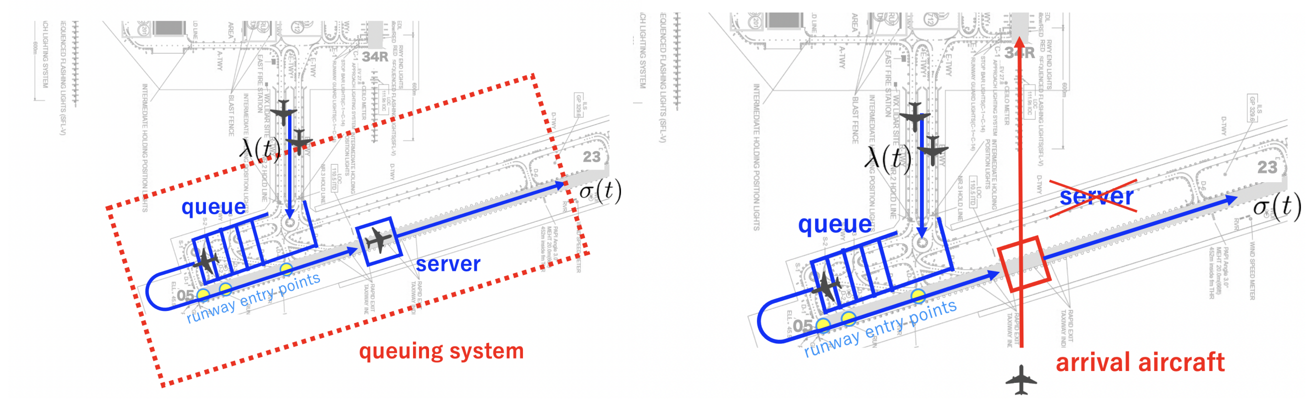

(a) $S(t) = 1.0$ (b) $S(t) = 0$

Figure 7 – Modeling the RJTT runway 05 departure queue.

3.2 Time-Varying Fluid Queue

In this section, we formulated the $G(t)/GI/s(t)$ aircraft departure queue based on Whitt et.al. [6, 7] and Eri et. al.[8].

Firstly, we defined $\Lambda(t)$. This is the sum total of the departure traffic, that is, input into the queuing model over the time interval $[0,t]$, which is as follows with $t \geq 0$ as the arrival rate for $\lambda(t)$ integration.

$$\Lambda(t) \equiv \int_0^t \lambda(u)du \tag{1}$$

Secondly, the cumulative distribution function (CDF) for service time $G(x)$ is an integration of the probability density function (pdf) for service time $g(u)$ when $x \geq 0$.

$$G(x) = \int_0^x g(u)du \tag{2}$$

Here, $\bar{G}(x)$ and $h_G(x)$ are defined as follows.

$$\bar{G}(x) \equiv 1 - G(x) \tag{3}$$

$$h_G(x) \equiv \frac{g(x)}{\bar{G}(x)} \tag{4}$$

Next, we determined two key performance descriptors $B(t)$ and $Q(t)$. Time-varying function $B(t)$ is the quantity of flow in service at time t, and $Q(t)$ is also a time-varying function indicating the quantity of flow waiting in the queue at t.

Firstly, we defined $B(t)$. The quantity of flow in service at time t, with service in progress for time $y \geq 0$, $B(t,y)$, is defined as follows.

$$B(t,y) = \int_0^y b(t,x)dx \tag{5}$$

Here, $B(t) \equiv B(t,\infty)$.

Secondly, we defined $Q(t)$. The quantity of flow waiting in the queue at t, which has been in the queue for time $y \geq 0$, $Q(t,y)$ is defined as follows.

$$Q(t,y) = \int_0^y q(t,x)dx \tag{6}$$

Here, $Q(t) \equiv Q(t,\infty)$. Next, $X(t)$ was determined as the total quantity of the flow in the queuing system at t, and defined as follows.

$$X(t) = B(t) + Q(t) \tag{7}$$

Using Equations 5 and 6, the initial conditions $B(0,y)$ and $Q(0,y)$ depend on the densities $b(0,x)$ and $q(0,x)$.
With the above descriptions, the $G(t)/GI/s(t)$ model is composed of the five functions: $\lambda(t)$, $s(t)$, G, $b(0,\cdot)$, $q(0,\cdot)$.

3.3 Conditions of Flow in the System

In the queuing system, there are two types of situations, $Q(t) = 0$ or $Q(t) > 0$. We named $Q(t) = 0$ the "Underload (UL) condition" and $Q(t) > 0$ the "Overload (OL) condition." This section describes the details of the two conditions.

3.3.1 UL condition

In the UL condition, one of the key performance descriptors is $Q(t) = 0$, and we want another key output $B(t)$. In addition, we would like to know when UL changes to the OL condition. We defined this point as T_2.
Firstly, $B(t)$ can be determined as follows using equations. 1, 2, 3, and 5.

$$\begin{aligned} B(t) &= \int_0^t \bar{G}(x)\lambda(t-x)dx + \int_0^\infty \frac{\bar{G}(x+t)}{\bar{G}(x)} b(0,x)dx \\ &\leq \Lambda(t) + B(0) \end{aligned} \tag{8}$$

Assuming that there is no initial quantity in service, $B(0) = 0$, which when plugged into equation 8 gives the following.

$$B(t) = \int_0^t \bar{G}(x)\lambda(t-x)dx \tag{9}$$

Secondly, we determined T_2 using $B(t)$ as defined in equations 8 and 9. The results showed that the UL condition begins at time t_2 when 1) $B(t_2) < s(t_2)$ or 2) $B(t_2) = s(t_2)$, $Q(t_2) = 0$ and $\lambda(t_2) \leq s'(t_2) + \sigma(t_2)$, where $s'(t_2) = ds(t_2)/dt$. The UL condition ends at time T_2, switching to the OL condition. T_2 is defined as follows.

$$T_2 \equiv \inf\{u \geq t_2 : B(u) = s(u) \text{ and } \lambda(u) > s'(u) + \sigma(u)\} \tag{10}$$

Here, the quantity of flow finishing service and leaving the queuing system at time u, $\sigma(u)$ in equation 10 is defined as follows when $t \geq 0$.

$$\sigma(t) \equiv \int_0^\infty b(t,x)h_G(x)dx \tag{11}$$

In eq. 11, $b(t,x)$ is defined as follows.

$$b(t,x) = \begin{cases} \bar{G}(x)\lambda(t-x), \ x \leq t \\ \\ \frac{\bar{G}(x)}{\bar{G}(x-t)} b(0,x-t), \ x > t \end{cases} \tag{12}$$

In particular, if $b(0,\cdot) = 0$, which means that the input flow in service at $t = 0$ is 0, $b(t,x)$ is defined as follows when $x \leq t$.

$$b(t,x) = \bar{G}(x)\lambda(t-x) \tag{13}$$

Consequently , T_2 is defined by equation 10 in combination with equation 11, 12 or 13.

3.3.2 OL condition

In the OL condition, we want three outputs: (i) $Q(t)$, one of the key performance descriptors, (ii) T_1, which is defined as the point when the OL condition switches to the UL condition, and (iii) $v(t)$, which is defined as the "potential waiting time" of the fluid queue.
Firstly, $Q(t)$ is defined as follows during the OL condition.

$$\begin{aligned} Q(t) &= \int_0^t \lambda(t-x)dx + \int_0^\infty q(0,x)dx \\ &\leq \Lambda(t) + Q(0) \end{aligned} \tag{14}$$

Assuming that there are no aircraft in the waiting room initially, $Q(0) = 0$, which yields the following when plugged into equation 14 .

$$Q(t) = \int_0^t \lambda(t-x)dx \tag{15}$$

Secondly, we determined T_1, the time the OL condition terminates and switches to the UL condition, using $Q(t)$ as define by equations 14 or 15. On the assumption that the OL condition starts at time t_1 when 1) $Q(t_1) > 0$ or 2)$Q(t_1) = 0$, $B(t_1) = s(t_1)$ and $\lambda(t_1) > s'(t_1) + \sigma(t_1)$. T_1 is defined as follows.

$$T_1 \equiv \inf\{u \geq t_1 : Q(u) = 0 \text{ and } \lambda(u) \leq s'(u) + \sigma(u)\} \tag{16}$$

$\sigma(u)$ is equivalent in equations 16 and 11. $b(t,x)$ in the OL condition is defined as follows.

$$b(t,x) = \begin{cases} \bar{G}(x)b(t-x,0), \ x \leq t \\ \\ \frac{\bar{G}(x)}{\bar{G}(x-t)}b(0,x-t), \ x > t \end{cases} \tag{17}$$

In equation 17, $b(t,x) = b(t,0)$ when $x = 0$. $b(t,0)$ is defined as follows.

$$\begin{aligned} b(t,0) &= s'(t) + \sigma(t) \\ &= s'(t) + \int_0^\infty b(t,x)h_G(x)dx \\ &= s'(t) + \int_0^\infty \frac{b(0,y)g(t+y)}{\bar{G}(y)}dy \\ &\quad + \int_0^t b(t-u,0)g(u)du \end{aligned} \tag{18}$$

Thirdly, we defined $v(t)$ as follows when $t \geq 0$.

$$v(t) \equiv \inf\{u \geq 0 : E(t+u) - E(t) \geq Q(t)\} \tag{19}$$

In equation 19, $E(t)$ is the quantity of flow entering service during time interval $[0,t]$, and it is defined as follows when $t \geq 0$.

$$E(t) \equiv \int_0^t b(u,0)du \tag{20}$$

In equation 20, $b(u,0)$ is defined by equation 18.

3.4 Aircraft Departure Waiting Time

In this paper, we defined aircraft departure waiting time as $v_{dp}(t) = v(t)$ in equation 19.
In addition, we considered another descriptor W_{dp} to approximate the total waiting time of departure aircraft during the estimation time period including m times OL periods. We defined W_{dp} as follows.

$$W_{dp} \equiv \sum_{i=1}^{m} \bar{v}_{dp,i} n_i \tag{21}$$

In eq. 21, $\bar{v}_{dp,i}$ is the mean of $v_{dp}(t)$ during the i th OL period. n_i is the number of departure aircraft entering the system during the i th OL period.

4. Estimating Departure Queues

4.1 Stochastic Features in the Queuing Model

4.1.1 Arrival Rates

In this section, we analyzed a day of departure operations at RJTT runway 05 using the departure queue model described above. We examined stochastic features of operations on November 15th, 2019 by using the same methods and data, which will be described later, as a previous paper [8]. This study also considered how much impact arrivals on runway 34R have on departure traffic.
Aircraft arrival rate $\lambda(t)$ is the number of departure aircraft passing the point 0.5 NM away from the runway entry points in an hour.From the perspective of queuing system, this is the number of departures entering the queuing model. The arrival rate is given as an average for each 10-minute interval in this case study. Figure. 8 shows $\lambda(t)$ as time-varying in 10-minute intervals throughout the day, although the maximum runway throughput is fixed at 28 departures per hour.

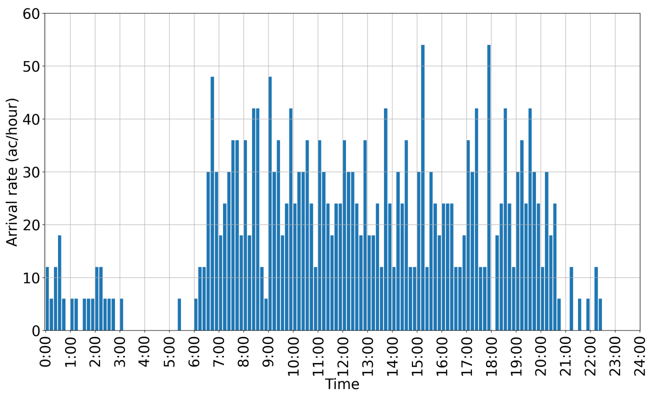

Figure 8 – Arrival rate at the queuing system. [8]

4.1.2 Service Time

In this model, service time is defined as the sum of ROT and separation time at the runway entry points. A service time histogram constructed using actual traffic data is shown in Figure 9. It's important to note that ROT includes the effects of runway 34R arrivals with their actual arrival rate, because we did not separate ROT into runway 34R arrival impact and other factors. In addition, these determinations are made using only service time shorter than 200 s in this study because the departure separation grows wider when the departure rate at the runway is low. Figure 10 shows a CDF of service time, $G(x)$. We use stochastic distribution to estimate states and waiting times of the departure queues in the following section.

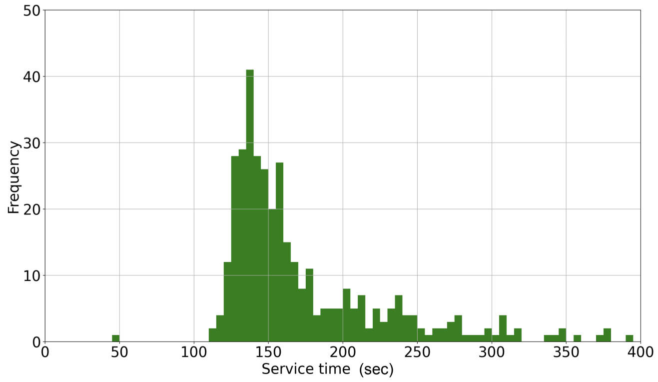

Figure 9 – Service time. [8]

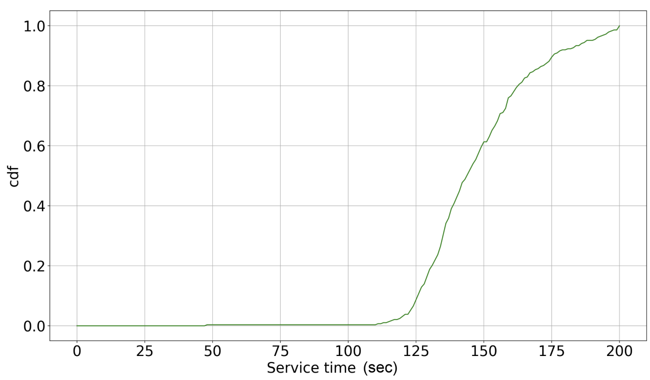

Figure 10 – CDF of service time, $G(x)$ [8]

4.2 Modeling Arrival Traffic Interference

In this section, we describe a method for describing about $s(t)$, the number of departure aircraft allowed to use the runway. As previously stated, runway 05 is only used for departure traffic and service times include the impact of runway 34R actual arrivals. Consequently, $s(t) = 1.0$ is used under actual runway 34R arrival rate conditions. In addition, we considered how $s(t)$ changes when the rate of runway 34R arrival is higher than actual data. Firstly, we defined the time r. r as the time interval between runway 34R arrivals reaching the point P_r and passing through the intersection of the runway 34R landing course and runway 05. Point P_r is a location on the runway 34R landing course and the farthest location at which runway 05 departure is restricted from starting to take off when runway 34R arrivals are flying over. Secondly, we considered runway 05 departure traffic behavior with runway 34R arrivals. Assuming that departure traffic is ready to start its take-off roll at the exact time arrival traffic reaches point P_r, departure traffic will wait for time r. In other words, service will be stopped for time r in the departure queuing model. This means that $s(t) = 0$ for time r. On the other hand, departure traffic will not be delayed by arrival traffic in situations such as when running on the taxiway, entering the departure runway, or waiting on the runway due to a wake vortex. Departure traffic is impacted by arrival traffic for the first time at to takeoff. Thus, we estimated the mean of the time $\bar{r}$ for which departure traffic is impacted by arrival traffic, including the arrivals' influence on the departure queuing system.

Let T_s be service time for departure traffic. When $T_s \geq r$, the probability that departure traffic will be ready to take off during the time an arrival aircraft is flying between point P_r and the intersection with the runway 34R landing course and runway 05 is r/T_s. If departure traffic is affected by an arrival, the times of infimum and supremum that departure cannot start takeoff are 0 and r. In addition, the distribution of departure-restricted time is uniform from 0 to r, In other words, the mean of departure restricted time is $r/2$. Hence, the overall average of departure restricted time $\bar{r}$ in service time T_s is defined as follows.

$$\bar{r} = \frac{r}{T_s} \times \frac{r}{2} = \frac{r^2}{2T_s} \tag{22}$$

When $T_s < r$, we can calculate $\bar{r}$ based on the above as follows.

$$\bar{r} = \frac{2r - T_s}{2}. \tag{23}$$

4.3 Impacts of Arrival Traffic Interference on the Departure Queue

To apply the impact of arrival traffic interference on the departure queue to the queuing model, we determined the distance of P_r from runway 05 and the value of r as follows. Initially, we fixed the distance of P_r from runway 05. Based on interviews with some air traffic controllers, 3.5 NM from runway 05 was determined adequate for the distance P_r. Thus, we positioned P_r on the runway 34R arrival course 3.5 NM from runway 05. Furthermore, the distance between the runway 05 and runway 34R threshold is about 1.5 NM. Therefore, the threshold for the distance between P_r and runway 34R is about 5.0 NM. Next, we calculated the value of r. A speed restriction of 160 kt is published on runway 34R 5.0 NM from the final ILS approach, so we set the arrival aircraft speed at P_r as 160 kt. In addition, we set the threshold for arrival aircraft speed at runway 34R as 140 kt.

This is an attribute for which most regular passenger aircraft flights at RJTT are classified in approach category C or D. Moreover, the approach category C and D boundary speed threshold is 140 kt. As a result, we calculated $r \fallingdotseq 95$ from the speed of the aircraft and distance P_r. Following our previous discussion, we considered how to apply the influence of arrival traffic to the departure queue specifically. Regarding $\bar{r}$, service time is given by a distribution, thus, we can calculate $\bar{r}$ for each service time. We used the mean $\bar{r}$, which it is about 31.1 seconds, with actual data for evaluation of the queuing model. In this paper, statistical verification is planned for understanding the impact of arrival traffic. Thus, we distributed the decrease of $s(t)$ to a wide time frame. In the case of one arrival exceeding the actual data value, 30 minutes, s(t) for 30 minutes is about 0.983, whereas the time for $s(t) = 0$ is about 31.1 seconds. In addition, we set $s'(t) \equiv 0$ because variation of $s(t)$ is sufficiently small from the above discussion.

4.3.1 Time-Varying States in the Departure Queue

Using the stochastic features in Section 4.1 this section estimates the time-varying states $B(t)$ and $Q(t)$. Simultaneously, we obtained the ith OL starting time $t_{1,i} = T_{2,i}$, termination time $T_{1,i}$, and their time intervals $T_{1,i}$ and $t_{1,i}$.

First, Figure 11 shows the results for estimating time-varying states for the departure queue in a single day with $s(t) \equiv 1.0$. Naturally, the result is the same as previous paper [8]. A total of 21 OL periods times are counted. During the OL periods $B(t) = s(t)$ and $Q(t) > 0$ as shown in Figure 11. Given that $\lambda(t)$ is the average arrival rate in a 10-minute time interval, the values of $B(t)$ and $Q(t)$ are also given as the average for every 10 minutes. The maximum $Q(t)$ value is 1.22, which means that 1.22 departures are waiting in the departure queue for 10 minutes on average.

Next, we obtained the results for estimates of time-varying states for the departure queue in a day under $s(t) = 0.983$ when $54,000 \leq t \leq 55,800$. These conditions mean that one more arrival is landing on runway 34R in the time between 54,000 and 55,800 than in the actual data. The results of analysis are described in the next section, along with comparisons to the queuing model results with different $s(t)$ conditions.

4.3.2 Comparing Departure Waiting Time in the Queue

In this section, we compared the departure waiting time in the queue with different $s(t)$ values.

Table 1 summarizes the result of analysis with $s(t) \equiv 1.0$, the value of the ith OL time intervals $T_{1,i} - t_{1,i}$, the aircraft departure waiting time $v_{dp,i}$ and total aircraft departure waiting time in the intervals. The maximum OL time interval is estimated to be 1950 seconds in the 7th OL interval between 10:00 and 1:00 a.m. (because $T_{1,7} = 38,559$ corresponds to 10:42:39 a.m.). The maximum departure waiting time average in a 10-minute interval was 82 seconds in the 14th and 17th OL intervals, which occurred between 15:00 and 19:00 ($T_{1,14} = 55,305$ and $T_{1,17} = 64,882$). As stated in previous paper

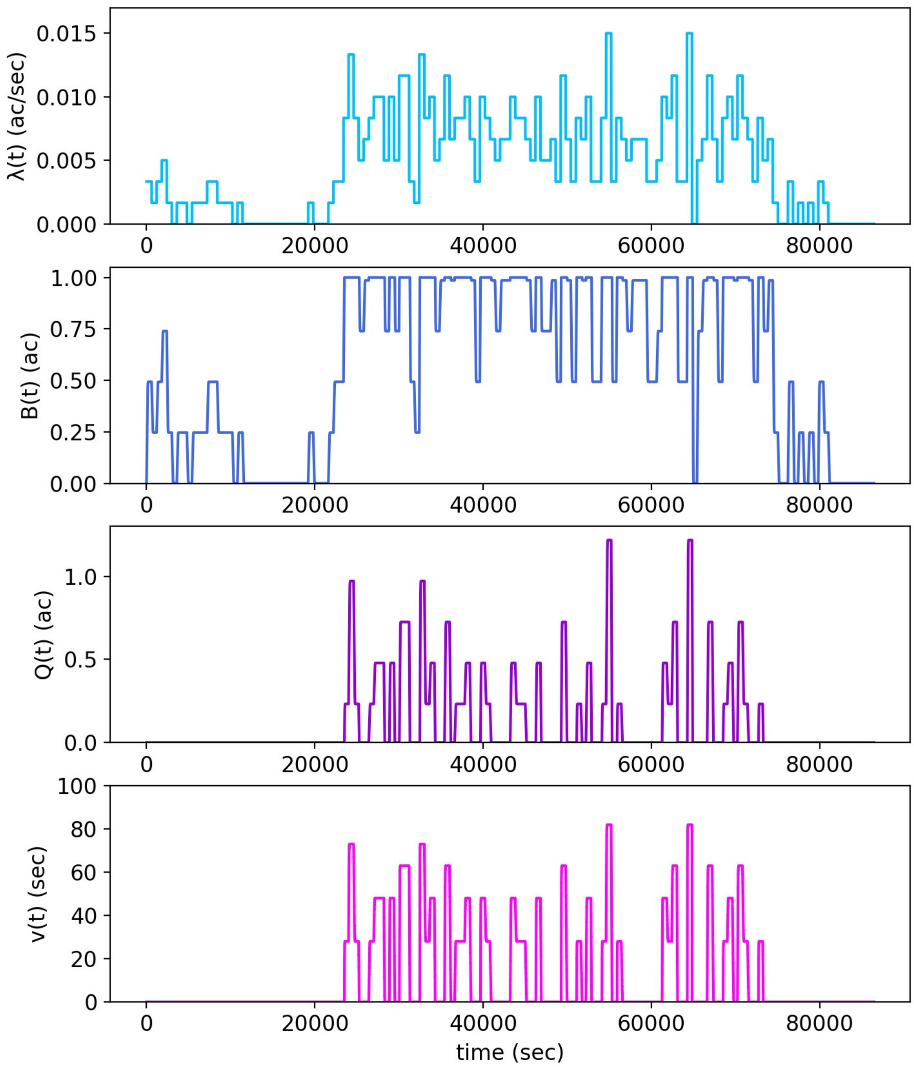

Figure 11 – Time-varying states in the departure queue, $\lambda(t)$, $B(t)$, $Q(t)$, and $v(t)$ in the ith OL period for a single day.

[8], the proposed model enables us to estimate the aircraft departure waiting time in the queue and the OL start and end times.
The total aircraft departure time in Equation (21), W_{dp}, is given as the sum of $W_{dp,i}$ in Table 1. W_{dp} = 9030 (seconds) $\approx$ 2.5 (hours) for the day.

Table 1 – OL time intervals and departure waiting times for a single day

i	$T_{1,i}$ **(s)**	$T_{1,i}-t_{1,i}$ **(s)**	$max.v_{dp,i}$ **(s)**	n_i **(Aircraft)**	$W_{dp,i}$ **(s)**
1	25,270	1768	73	17	734
2	28,296	1887	48	16	627
3	29,496	643	48	5	213
4	31,288	1248	63	13	774
5	34,296	1831	73	18	869
6	36,166	763	63	8	415
7	38,559	1950	48	14	454
8	40,947	1270	48	10	351
9	45,147	1942	48	17	553
10	46,896	643	48	7	298
11	49,966	705	63	6	321
12	51,747	645	28	5	121
13	52,872	667	48	6	252
14	55,305	1203	82	10	542
15	56,547	645	28	6	145
16	63,088	1835	63	16	716
17	64,882	638	82	6	418
18	67,366	763	63	5	259
19	69,759	1257	48	9	322
20	71,547	1344	63	13	541
21	73,270	568	28	4	103

Furthermore, the table below shows the result of the queuing model with other $s(t)$ values.
Table 2 summarizes the results of analysis with $s(t)$ values reflecting the impact of additional (1-3 aircraft) runway 34R arrivals when $36,600 \leq t \leq 38,400$ (including almost all of the maximum OL time interval, the 7th OL time interval). Comparison with the analysis with $s(t) \equiv= 1.0$, showed that only the 7th OL time result was different, so the table shown summarizes of the 7th OL time interval. **a** is a the number of additional aircraft compared to actual data.
Table 3 summarizes the result of analysis with $s(t)$ that reflect the arrival impact of the same number of aircraft as the above analysis when $54,000 \leq t \leq 55,800$ (including the time interval with maximum departure waiting time for 10-minute average, the 14th OL time interval). In comparison with the analysis with $s(t) \equiv 1.0$, only the 14th OL time result is different, so the table shown summarizes results for the 14th OL time interval.
In the results of both analyses, W_{dp} grows with increases to the number of additional arrival aircraft. This means that the model estimates that aircraft departing from runway 05 experience more and more waiting time in the day with more arrival aircraft added.

Table 2 – Variation of OL time and watiing times with changing $S(t)$ between 38,400 and 40,200.

a (Aircraft)	$T_{1,7}-t_{1,7}$ **(s)**	$max.v_{dp,7}$ **(s)**	n_7 **(Aircraft)**	$W_{dp,7}$ **(s)**	W_{dp} **(s)**
0	1950	48	14	454	9030
1	1958	50	14	478	9055
2	1958	52	14	512	9089
3	1958	54	14	538	9115

Table 3 – Variation of OL time and waiting times with changing $S(t)$ between 54,000 and 55,800.

a (Aircraft)	$T_{1,14} - t_{1,14}$ (s)	$max.v_{dp,14}$ (s)	n_{14} (Aircraft)	$W_{dp,14}$ (s)	W_{dp} (s)
0	1203	82	10	542	9030
1	1208	83	10	555	9044
2	1213	84	10	572	9061
3	1218	85	10	585	9074

5. Discussion

In this paper, we proposed a departure aircraft queuing model for the impact of arrival aircraft, specifically aircraft landing on another runway. The proposed model enables us to estimate the aircraft departure waiting time in the queue and the OL start and end times, even if arrival aircraft rates are higher than actual data. For integrating arrival and departure runway operation, we need to think about improvements to the model for (1) arranging ideal arrival rates in the queuing system and (2) reflecting the impact of arrivals on the same runway. In particular, we think the idea of arrival traffic interference for departure of other runways can be applied to the arrival aircraft impact for same runway departure. For example, departure traffic is impacted by arrival traffic for the first time at to enter runway, and so on.

6. Conclusions

This study proposed an aircraft departure model at a runway using a time-varying fluid queue with time-varying for the number of servers. The proposed model enables us to design departure traffic flow with arrival traffic for related runways and evaluate the impact of the arrival traffic on departures by assessing the waiting time in the queue. As a case study, the fluid queue model was successfully implemented into the aircraft departure queue at runway 05 of Tokyo International Airport. The results showed that waiting time grows with the increases to the number of arrival aircraft.

This paper developed a methodology to model departure queues with arrival traffic landing on related runways. In future studies, the authors plan to further develop the departure queue model and validation method and examine the best departure metering approach, which is applicable in the actual airport operations and system design. More specifically, we have two issues: (1) arranging ideal arrival rates in the queuing system and (2) developing a departure queuing model for reflecting the impact of arrivals on the same runway. This will enable us to discuss future integrated control of arrival and departure management.

7. Acknowledgements

This research was supported by a Grant-in-Aid for Scientific Research (20H04237). We would like to express our sincere appreciation for the data and technical support provided by the Civil Aviation Bureau of the Ministry of Land, Infrastructure, Transport and Tourism.

References

[1] FAA Surface CDM Team. US Airport Surface Collaborative Decision Making (CDM) Concept of Operations (ConOps) in the Near-Term: Applications of Surface CDM at United States Airports. 2012.

[2] EUROCONTROL Airport CDM Team. Airport CDM Implementation-The Manual. 2018.

[3] S. Badrinath and H. Balakrishnan and E. Joback and T. Reynolds. Impact of Off-Block Time Uncertainty on the Control of Airport Surface Operations. *ATransportation Science*, 54(4), pp.855-1152, 2020.

[4] I. Simaiakis and H. Balakrishnan. A queuing model of the airport departure process. *ATransportation Science*, 50(1), pp.94-109, 2015.

[5] S. Badrinath and MZ. Li and H. Balakrishnan. Integrated surface–airspace model of airport departures. *AJournal of Guidance, Control, and Dynamics*, 42(5), pp.1049-1063, 2018.

[6] Y. Liu and W. Whitt. The $G_t/GI/s_t + GI$ many-server fluid queue. *Queuing System*, 71, pp.405-444, 2012.

[7] W. Whitt. Time-Varying Queues, *A Queuing Models and Service Management*, 1(2), pp.79-164, 2018.

[8] E. Itoh, M. Mitici and M. Schultz. Modeling Aircraft Departure at a Runway using a Time-varying Fluid Queue. *Aerospace*, 9(3) 119, 2022.

[9] R. Shone, K. Glazebrook and K. Zografos. Applications of Stochastic Modeling in Air Traffic Management: Methods, Challenges and Opportunities for Solving Air Traffic Problems Under Uncertainty. *European Journal of Operational Research*, 292(1), pp.1-26, 2021.

[10] E. Itoh and M. Mitici. Queue-based Modeling of the Aircraft Arrival Process at a Single Airport. *Aerospace*, 6(10), 103, 2019.

[11] E. Itoh and M. Mitici. Analyzing Tactical Control Strategies for Aircraft Arrivals at an Airport Using a queuing Model. *Journal of Air Transport Management*, 89, 101938, 2020.

[12] E. Itoh and M. Mitici. Evaluating the Impact of New Aircraft Separation Minima on Available Airspace Capacity and Arrival Time Delay. *The Aeronautical Journal*, 124(1274), pp.447-471, 2020.

[13] K. Sekine and F. Kato and K. Kageyama and E. Itoh. Data-Driven Simulation for Evaluating the Impact of Lower Arrival Aircraft Separation on Available Airspace and Runway Capacity at Tokyo International Airport. *Aerospace*, 8(6), 165, 2021.

[14] Airports Council International (ACI). Passenger Traffic 2017 FINAL (Annual). In *Passenger Summary*, Airports Council International, Montreal, QC, Canada, 2019.

[15] Ministry of Land, Infrastructure, Transport and Tourism. AIS Japan—Japan Aeronautical Information Service Center. 2021. Available online: `https://aisjapan.mlit.go.jp` (accessed on 24 May 2022).

8. Contact Author Email Address

mailto: { eriitoh, iwata-d36cw }@g.ecc.u-tokyo.ac.jp

9. Copyright Statement